Deconstruction via adsorbate-driven ordering: O-W(001)

K. Grzelakowski, I. Lyuksyutov,* and E. Bauer
Physikalisches Institut, Technische Universität Clausthal, D3392 Clausthal-Zellerfeld, Germany
(Received 8 July 1991; revised manuscript received 12 November 1991)

The phase transition from the $p(2\times1)$ to the (1×1) structure in the O-W(001) system and its critical behavior is studied. Above the critical temperature of the $p(2\times1)$ structure ordering into a (1×1) structure is observed. A model for the anomalous ordering and critical behavior is proposed.

I. INTRODUCTION

Surface-reconstruction phenomena have attracted great attention in recent years both from experimentalists and theoreticians. A rich variety of phase transitions was found, and many microscopic models have been proposed to describe them. Reconstruction takes place on clean and adsorbate-covered surfaces. One of the most studied is the W(001) surface. This surface exhibits a variety of structural phase transitions with temperature in the clean state and in the presence of various adsorbates, which were extensively investigated during the past decade. Most studies have been concerned with the clean W(001) surface and with the hydrogen- or oxygen-induced surface reconstruction.

Oxygen on W(001) is a complex system with many phases of which the $p(2\times1)$ structure at a coverage of $\Theta=\frac{1}{2}$ has been studied in much detail.[1-3] This structure has a reversible phase transition into a (1×1) structure, in which both substrate and adsorbate atoms are involved. It is generally accepted that, at temperatures far below T_c, every second row of tungsten atoms along one of the two [100] directions is missing in the topmost layer.[1] This picture is supported by low-energy ion-scattering (LEIS) measurements,[2] which are known to be sensitive to the local atomic arrangement in the topmost layer. The oxygen atoms in the missing row model are adsorbed at the bottom of the troughs between the W rows.[3] With increasing temperature the oxygen atoms move increasingly outward. This follows from the increase of the work function and of the O^+ electron-stimulated-desorption (ESD) yield with temperature.[3] One interesting aspect of this phase transition is that the tungsten atoms have to be transported over large distances to produce the missing row structure.[3] In contrast, in the case of the clean or hydrogen-induced surface reconstruction the top layer atoms are only slightly shifted from their bulk positions.

There is an indication that the high-temperature (1×1) phase is particularly well ordered. In this work we have investigated the $p(2\times1)\leftrightarrow(1\times1)$ deconstruction phase transition with a high-resolution low-energy electron-diffraction (LEED) apparatus and found unusual critical behavior and ordering phenomena. We propose a simple model based on oxygen-induced changes in the tungsten-tungsten interactions in order to explain these unusual observations.

II. EXPERIMENTAL PROCEDURE

The experiments were carried out with an UHV low-energy electron diffractometer[4] which consists of three parts: a movable and finely adjustable electron gun, a high-precision crystal manipulator, and a 127° energy analyzer. The electron gun with an energy spread of 0.4 eV was routinely operated between 20 and 120 eV at typically 3×10^{-9} A beam current. The precision crystal holder had a polar and azimuthal angular accuracy of 3×10^{-4} and 9×10^{-4} rad, respectively. The 127° energy analyzer had an energy resolution better than 0.4% and electrons were detected with a channeltron. One of the most important features of the system is its wide dynamic range of 10^5.

The surface orientation of the tungsten single crystal was within 0.05° of the (001) plane. The crystal was cleaned by careful heating in oxygen in the 10^{-6}-mbar range and subsequent flashing in UHV until impurity Auger signals were below their detection limits ([W]:[O]=200, [W]:[C]=300). During measurement the base pressure was kept below 4×10^{-11} mbar and even during flashing to 2300 K the pressure stayed in the 10^{-11} range. Heating to temperatures above 700 K was accomplished by electron bombardment of the back side of the tungsten support disc of the W(001) crystal. To avoid the influence of the heating current on measurements both the filament current and the accelerating potential were chopped with a 22-ms period (10 ms heating, 10 ms counting, 2 ms neutral range). The temperature was recorded using a W–5 at.% Re/W–26 at.% Re thermocouple spotwelded to the front side of the crystal. High-purity oxygen (99.9999%) was adsorbed at 700 K using a tube-type molecular beam source starting at a base pressure of 4×10^{-11} mbar. The typical oxygen pressure and exposure time required to obtain a coverage of $\frac{1}{2}$ monolayer (ML) were 9×10^{-10} mbar and 900 s, respectively. After every exposure the sample was annealed at 1300 K for 1 min.

III. EXPERIMENTAL RESULTS AND DATA ANALYSIS

A. Deconstruction ordering

Figure 1 shows the temperature dependence of the intensity of the specular beam (at 87 eV and 59° angle of incidence) for a coverage of $\Theta=\frac{1}{2}$. One can see three

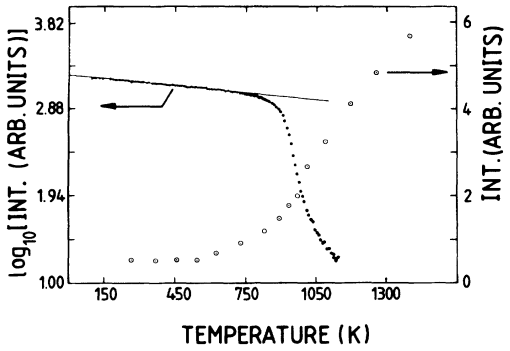

FIG. 1. Temperature dependence of $(0\frac{1}{2})$-spot intensity (dots) and (00)-spot intensity (circles) of the $p(2\times1)$ structure at $\frac{1}{2}$ monolayer of oxygen.

characteristic regions: between 150 and 700 K a Debye-Waller (DW) behavior with a DW factor of 4.1×10^{-4} corresponding to a Debye temperature of 214 K, between 700 and 800 K a behavior attributed to changes in the frozen-in domain walls distribution,[5] and a third region above 800 K, the region of the $p(2\times1)\leftrightarrow(1\times1)$ phase transition. In this last range the intensity of the specular beam increases more then tenfold. Because of the small scattering factor of oxygen these changes have to be connected with changes in the pair-correlation function of the tungsten atoms.

The character of the rearrangement of the tungsten atoms during the phase transition is more evident in out-of-phase measurements of the (01) spot profile in the [100] direction far above T_c(1230 K). The spot profile cannot be explained by two symmetrically placed satellites only, but also has a strong central component which is an indication of a random terrace size distribution.[6] A fit of such a profile by a sum of a Gaussian for the central Bragg component and two Lorentzians convoluted with the instrument response function is shown in Fig. 2. The distance between the satellites in Fig. 2(a) corresponds to about 150 Å in the real space. In general the splitting not only depends upon the mean terrace width but also upon the details of the terrace width distribution about its mean value.[6] For comparison with Fig. 2(a), Figs. 2(b) and 2(c) show the (01) spot profiles of the clean (1×1) surface and of the $p(2\times1)$ structure at $\frac{1}{2}$ ML of oxygen, respectively, both measured at room temperature under the same experimental conditions. The most striking features here are the similarities between the curves, in particular between Eqs. 2(a) and 2(b) and the much smaller splitting in Fig. 2(c) than in Fig. 2(a). The lack of noticeable differences in the line shapes of the integral order spots from the clean and oxygen-covered surface was found also in reflection high-energy electron diffraction experiments.[7] In all three cases the peak splitting can be attributed to a geometrical step distribution with a lower cutoff.[6] This is supported by the Lorentzian-like line shapes of the fractional order spots, which is a well-known feature of a geometrical step distribution.[8] It is important to mention that the fractional order spots never split at any energy while the integral order spots split at certain energies due to the presence of steps on the surface. This phenomenon has the same origin as the non-splitting of the superlattice reflection of the reconstructed clean W(001) surface.[9] Following Lu and Wang[10] we attribute this striking phenomenon to equal population of in-phase and antiphase relationships amongst the $p(2\times1)$ domains nucleated at random positions on the surface. The half width of the angular profile of the fractional order spots reflects the average size of the $p(2\times1)$ domains. The FWHM of the $(0\frac{1}{2})$ reflection from a well-ordered $p(2\times1)$ structure at $\Theta=\frac{1}{2}$ corresponds to about 270 Å in real space, which is in good agreement with the value 280 Å obtained from the splitting of the (01) spot in Fig. 2(c).

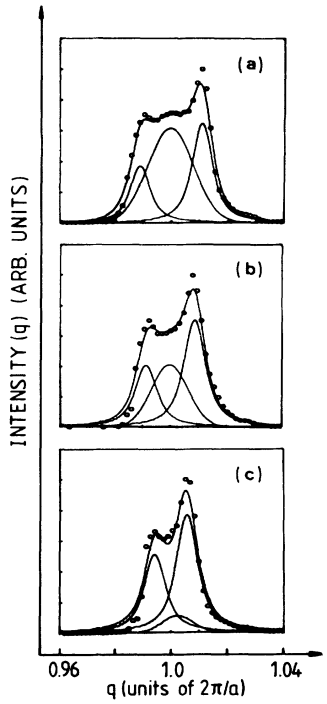

FIG. 2. Experimental (0 1) spot profiles at 55 eV for (a) an oxygen-covered surface at 1230 K, (b) a clean surface at room temperature, and (c) an oxygen-covered surface at room temperature. Oxygen coverage is $\frac{1}{2}$ monolayer.

Figure 3 shows three in-phase (01) spot profiles at a beam energy of 25 eV and an angle of incidence of 59°. The half width of the angular profile in Fig. 3(c) corresponds to a coherence length of about 1000 Å.

B. Critical behavior

Although a large number of studies of the system O-W(001) have been made up to now, none of them investigated the problem of the complexity of the $p(2\times1)\leftrightarrow(1\times1)$ phase transition. Whereas the structure of the $p(2\times1)$ surface and its properties below T_c are relatively well known,[1-3] the character of the phase transition and of the high-temperature (1×1) phase are not clear. The temperature dependence of the intensity of the $(0\frac{1}{2})$ reflection at $\Theta=\frac{1}{2}$ (Fig. 1) starts to deviate from the Debye-Waller behavior at 700 K, 200 K below T_c. T_c and the critical exponent β of the order parameter were

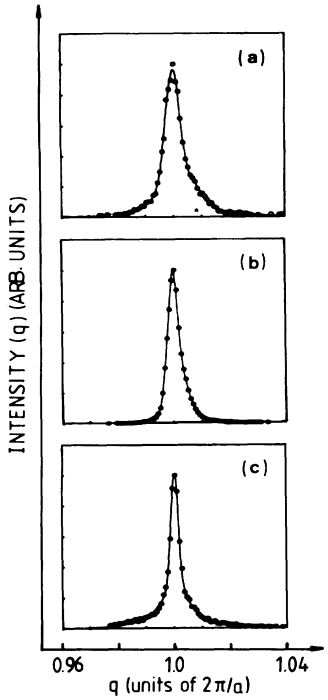

FIG. 3. Experimental (0 1) spot profiles at 25 eV for (a) an oxygen-covered surface at 1230 K, (b) a clean surface at room temperature, and (b) an oxygen-covered surface at room temperature. Oxygen coverage is $\frac{1}{2}$ monolayer.

determined from the relationship $I(\tau)\sim\tau^{2\beta}$, τ being the reduced temperature $(T-T_c)/T_c$, following a simple method.[11] Varying T_c and the temperature range the best linear relationship between DW factor-corrected experimental intensities and reduced temperature τ on a log-log scale was determined. Then a one-parameter fit procedure was used to determine β. This two-step operation allowed us to locate T_c and β between 900 and 908 K and 0.057 and 0.068, respectively. The limit of the temperature range in which the power law is still satisfied is about 20 K below T_c.

Another method for the determination of T_c and β is based on an analysis of profile line shapes to extract information about the long-range order. This method is physically more appropriate then the first one because frozen-in fluctuations and short-range correlations can be easily excluded, but is usually restricted by experimental conditions to a small number of data points. Ideally the scattered intensity in the critical range consists of a δ function arising from long-range order and a correlation function attributed to fluctuations. In our LEED experiment the instrument response function $f(k)$ and the specimen transform the δ function into a Gaussian whose FWHM corresponds to 1000 Å in real space and the correlation function is nearly Lorentzian:

$$J(q,\tau)\sim\int dk[I(q_0,\tau)\delta(q-q_0-k)+\chi(q-q_0-k,\tau)]f(k)\ . \quad (1)$$

The amplitudes $I(q_0,\tau)$ extracted from the fit procedure were then used to calculate T_c and β. We assume that finite-size effects spread T_c into a Gaussian distribution, which transforms the power law into[11]

$$I(q_0,T)\sim\int_{T-T_c}^{+\infty}dt\left|\frac{T-T_c+t}{T_c}\right|^{2\beta}e^{-(1/2)t^2/\Delta t}\ . \quad (2)$$

This relationship was used to fit $I(q_0,\tau)$ for many values of Δt, with T_c and β as a free parameter. The rms deviation shows a sharp and single minimum at $\Delta t=9$ K for which $T_c=903\pm1$ K and $\beta=0.063\pm0.005$. The critical exponent η was extracted by a procedure described elsewhere.[12] In the kinematical approximation which is true for small q the correlation function is proportional to the scattered intensity and can be written in a general form as

$$G(q,\tau)=r_c^{2-\eta}f(qr_c)\sim J(q,\tau)\ . \quad (3)$$

[G is the correlation function, J the measured intensity, τ the reduced temperature, r_c the correlation radius, η the critical exponent, and $f(x)$ a universal function.] The universality of $f(x)$ for a given system and Eq. (3) lead directly to a simple scaling transformation, which above T_c allows a transformation of one spot profile into another arbitrarily chosen one in the following manner:

$$q'=\left[\frac{r_c'}{r_c}\right]q\ , \quad (4)$$

$$G'=\left[\frac{r_c'}{r_c}\right]^{2-\eta}G\ . \quad (5)$$

This procedure was applied to a number of DW-corrected spot profiles. A result for three experimental curves is shown in Fig. 4. The relatively good fit demonstrates the scale invariance on which Eqs. (4) and (5) are based and results in $\eta=0.53$.

In order to evaluate the critical exponents γ and ν we expand $G(q)^{-1}$ into a power series in q:

$$G^{-1}=1+a_1q^2-a_2q^4+a_3q^6-\cdots \quad (6)$$

and compare $G(q)$, after convolution with the instrumental response function, with measured angular spot profiles. The temperature dependence of $G(0,\tau)\sim|\tau|^{-\gamma}$

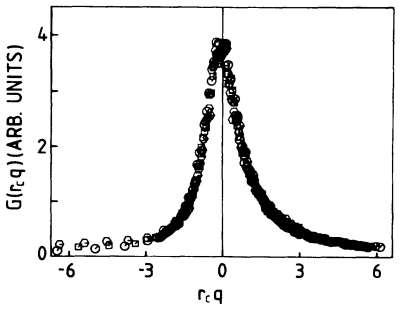

FIG. 4. Result of the scaling procedure applied to the correlation functions at 936 K (circles), 956 K (squares), and 975 K (hexagons) according to the transformations defined by Eqs. (4) and (5). ($0\frac{1}{2}$) superstructure spot. Oxygen coverage is $\frac{1}{2}$ monolayer.

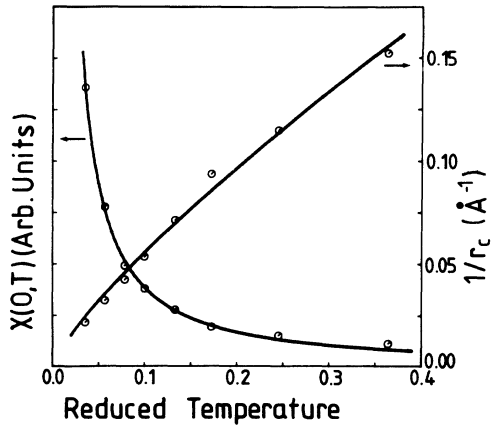

FIG. 5. Result of the fit procedure for extracting the critical exponents. Left side: temperature dependence of the amplitude of the correlation function, $\gamma=1.22\pm0.12$. Right side: temperature dependence of the reciprocal correlation length, $\nu=0.79\pm0.07$.

and $r_c(\tau)\sim|\tau|^{-\nu}$ extracted from this profile line-shape analysis gives directly γ and ν. The result of this procedure is shown in Fig. 5. The main source of error comes from the uncertainty in the relative temperature determination which is estimated to be 1 K at 1000 K. A comparison of the rms deviations for different fits of G, order parameter, and correlation length leads to the choice of 903 K as the best value of T_c. For this critical temperature a simple one-parameter fit gives $\beta=0.063\pm0.005$, $\gamma=1.22\pm0.12$, and $\nu=0.79\pm0.07$.

IV. MODEL

As mentioned above the experiment shows that the tungsten atoms form two lattices, $p(2\times1)$ and (1×1). Tungsten is a bcc crystal. In order to simplify the model we will consider in the following only the primitive cubic lattice. This simplification should not change the form of the phase diagram and the universality class. In the transition from the $p(2\times1)$ to the (1×1) lattice oxygen changes its position from the lower to the upper level. The simplest adsorption lattice for the topmost layer is shown in Fig. 6. In this model the tungsten atoms can occupy the vertices (circles) of the square lattice. Oxygen

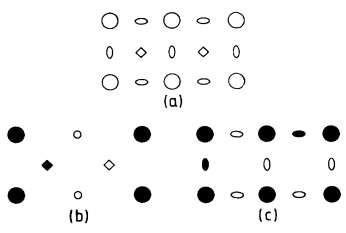

FIG. 6. (a) Tungsten atom positions and oxygen adsorption sites in a primitive cubic lattice model. Circles represent tungsten sites. Squares and ovals correspond to center and bridge adsorption sites. (b) and (c) are low- and high-temperature state occupations, respectively.

can occupy two kinds of states: the positions in the centers of the tungsten lattice (diamonds) and the short bridge positions (ovals) between the W sites (a). In the low-temperature state [$p(2\times1)$ structure] every second row of W sites and one of the center oxygen sites are occupied (b); in the high-temperature state all W sites are occupied and there are two statistically distributed O sites (c). Due to the high mobility of oxygen at and above the transition temperature we will consider it further as a lattice gas.

In the simplest model which can describe both the reconstructed and the unreconstructed surfaces only nearest (horizontal and vertical) site interactions and next-nearest (diagonal) site interactions between the tungsten atoms are assumed. It is convenient to discuss this problem in the magnetic model language. One can describe the presence or absence of tungsten atoms in the upper layer by up or down Ising spins, respectively. The mapping of the lattice-gas problem onto the magnetic model should be done with care. Usually, in lattice-gas models of chemisorbed layers the number of adsorbed particles is fixed. On the contrary, in magnetic models the magnetic moment is usually not fixed. Similarly, in the present case the number of tungsten atoms is also not fixed. In a three-level system the number of tungsten atoms in the upper layer can have in the thermodynamic limit (with equilibration time going to infinity) any value between 0 and $N_0/2$, N_0 being the number of atoms in the completely occupied layer, depending upon interaction constants and temperature. A one-dimensional example is illustrated in Fig. 7. The difference to the magnetic problem is that one has to create additional steps on the surface. But the total length of these steps should be of the order of the system size and is not significant in the thermodynamic limit. Actually in the real system, due to the limited mobility, there should be a finite density of steps, which is confirmed by experiment (see Sec. III A).

Let us return to the magnetic model. With the interactions mentioned above we have an Ising model on a square lattice with the Hamiltonian

$$H=J_1\sum_{\mathbf{a}_{NN}}S_{\mathbf{r}+\mathbf{a}_{NN}}+J_2\sum_{\mathbf{a}_{NNN}}S_{\mathbf{r}}S_{\mathbf{r}+\mathbf{a}_{NNN}}\,, \tag{7}$$

where the vectors $\mathbf{a}_{NN}$ and $\mathbf{a}_{NNN}$ are the nearest- and next-nearest-neighbor vectors. The ground state of this model is well known.[13,14] For $J_1<0$ and $J_2<-\frac{1}{2}J_1$ one

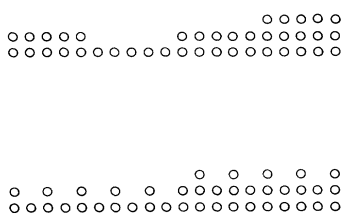

FIG. 7. Schematic cross section through the surface in the high-temperature state (top) which transforms into two terraces (bottom) in the transition to the reconstructed low-temperature state. Only W atoms are shown.

has a ferromagnetic state which corresponds to the unreconstructed surface, while the region $J_1 < 0$, $J_2 > -\frac{1}{2}J_1$ corresponds to an antiferromagnetic structure in the x or y direction. For $J_1 > 0$ other structures are possible. Actually one can add more complicated interactions in the model, e.g., a four-spin interaction:

$$J_3 \sum_{\mathbf{a}_i} S_{\mathbf{r}} S_{\mathbf{r}+\mathbf{a}_1} S_{\mathbf{r}+\mathbf{a}_2} S_{\mathbf{r}+\mathbf{a}_3} , \tag{8}$$

where the vectors $\mathbf{a}_i$ denote the vertices in one lattice cell. With this additional term the model (7) may be considered as a particular case of the 8-vertex or Baxter model with nonuniversal critical exponents. This model was studied numerically by many authors.[14,15] Figure 8 shows schematically part of the phase diagram of the model with the Hamiltonian (7). The general form of the phase diagram with the additional term (8) is the same in the region between $p(2\times1)$ and (1×1) phases (see, e.g., Refs. 14 and 15).

Upon heating the occupation of different adsorption sites by oxygen changes. In different adsorption sites oxygen influences the interaction between tungsten atoms in the top layer in different ways. A change in the oxygen concentration (in different occupation sites) therefore causes a change in the interaction between tungsten atoms. In the magnetic model language this means a change of the absolute and relative values of the interaction constants J_1, J_2, and J_3 in (7) and (8) with temperature.

A more general model to describe this reconstruction process can be constructed from the so-called restricted solid-on-solid model. The most recent form was introduced by Rommelse and den Nijs.[16] In this model the surface is described by columns of height $h(\mathbf{r})$ at each site $\mathbf{r}$ of a square lattice. Between neighboring vertices the column height can differ only by one lattice period. The interactions include nearest and next-nearest neighbors. Unfortunately the region of this model which is relevant to our system was not analyzed in Ref. 16.

V. DISCUSSION

The experimental data described in Sec. III show that at $T > T_c$ the (1×1) phase is apparently well ordered. The most important basis for this conclusion is that the half width of the specular beam is small and changes only slightly with temperature (Sec. III). The growth of the specular beam intensity also supports the picture of an ordered (1×1) phase. In the usual picture of reconstruction phase transitions it is implied that thermal fluctuations destroy the superstructure in the reconstructed phase and in this way restore the (1×1) symmetry. The well-ordered high-temperature phase which develops in the present system above the phase transition can be explained by the oxygen-driven interaction between tungsten atoms proposed above: the change of the oxygen positions with increasing temperature favors stronger interaction between the tungsten atoms and as a result the formation of a (1×1) structure. Simultaneously additional steps are created as indicated in Fig. 7 and the terrace size decreases by about a factor of 2.

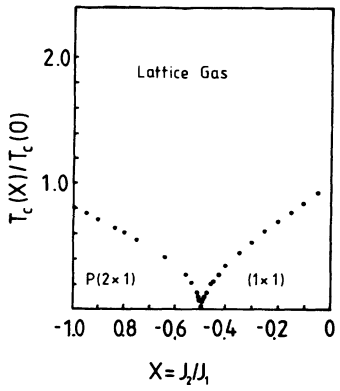

FIG. 8. Phase diagram for the model with Hamiltonian (7) (from Ref. 14). $x = J_2/J_1$, $J_1 < 0$.

In the models discussed in Sec. IV there is an intermediate disordered phase between the $p(2\times1)$ and (1×1) structures. As mentioned before, no evidence of such an intermediate phase was found in the experiment. Many explanations for this fact can be proposed. First, as can be seen from Fig. 8, the disordered region is very narrow for $J_2 \approx -\frac{1}{2}J_1$ and can simply correspond to the region with large fluctuations of the order parameter. Second, there can be a first-order phase transition close to the second-order phase transition between the phases $p(2\times1)$ and (1×1).[17,18] The reason for such a transition may be, e.g., a more complicated interaction. An interesting consequence of the conjecture of strong temperature-dependent interaction constants is that the real critical behavior will be masked by the rapid change of the interaction constants. In the 8-vertex version of the model considered here, the critical exponents change continuously with J_3. But J_3 itself can rapidly change with temperature in the phase-transition region. This may be an explanation of the unusual values of the critical exponents.

VI. CONCLUSIONS

We have found deconstruction ordering in the O-W(001) system. The experimental data can be understood on the basis of the oxygen-driven change in the tungsten adatom interactions.

ACKNOWLEDGMENTS

This work was supported by the SFB 126 Clausthal Göttingen. One of us (I.L.) acknowledges financial support by the Alexander von Humboldt Foundation and by the Ruhr Universität Bochum.

*Permanent address: Institute of Physics Kiev 252028 U.S.S.R.; present address: Fakultät für Physik und Astronomie, Theoretische Physik III Ruhr Universität Bochum, D-4630 Bochum, Germany.

[1]E. Bauer, H. Poppa, and Y. Viswanath, Surf. Sci. **58**, 517 (1976).

[2]D. R. Mullins and S. H. Overbury, Surf. Sci. **210**, 481 (1989).

[3]H. M. Kramer and E. Bauer, Surf. Sci. **92**, 53 (1980).

[4]W. Witt and E. Bauer, Ber. Bunsenges, Phys. Chem. **90**, 248 (1986); W. Witt, Ph.D. thesis, Technische Universität Clausthal, 1984.

[5]K. Grzelakowski and E. Bauer (unpublished).

[6]J. M. Pimbley and T. M. Lu, J. Appl. Phys. **57**, 1121 (1985); **58**, 2184 (1985); Surf. Sci. **159**, 169 (1985).

[7]B. J. Hinch, D. M. Rohlfing, J. Ellis, W. Allison, and R. F. Willis, Surf. Sci. **189/190**, 120 (1987).

[8]T.-M. Lu and M. G. Lagally, Surf. Sci. **120**, 47 (1982).

[9]M. K. Debe and D. A. King, Surf. Sci. **81**, 193 (1979).

[10]T.-M. Lu and G.-C. Wang, Surf. Sci. **107**, 139 (1981).

[11]G.-C. Wang and T.-M. Lu, Phys. Rev. B **31**, 9 (1984).

[12]K. Grzelakowski, I. Lyuksyutov, and E. Bauer, Phys. Rev. Lett. **64**, 32 (1990).

[13]N. W. Dalton and D. W. Wood, J. Math. Phys. **10**, 1271 (1969).

[14]M. Nauenberg and B. Nienhuis, Phys. Rev. Lett. **33**, 944 (1974); M. P. Nightingale, Phys. Lett. **59A**, 486 (1977); R. M. Swendsen and S. Krinsky, Phys. Rev. Lett. **43**, 177 (1979); M. N. Barber, J. Phys. A **12**, 679 (1979); **15**, 915 (1982).

[15]F. S. Rys, Phys. Rev. Lett. **51**, 849 (1983).

[16]M. den Nijs and K. Rommelse, Phys. Rev. B **40**, 4709 (1989).

[17]O. G. Mouritsen and A. J. Berlinsky, Phys. Rev. Lett. **48**, 181 (1982).

[18]T. L. Einstein, in *Chemistry and Physics of Solid Surfaces VII*, edited by R. Vanselow and R. F. Howe (Springer, Berlin, 1988).